APPLICATION OF BLUE LASER TRIANGULATION SENSORS FOR DISPLACEMENT MEASUREMENT THROUGH FIRE

MATTHEW S. HOEHLER AND CHRISTOPHER M. SMITH

Engineering Laboratory

National Institute of Standards and Technology

Gaithersburg, Maryland 20899 USA

(Corresponding author: matthew.hoehler@nist.gov)

Abstract

This paper explores the use of blue laser triangulation sensors to measure displacement of a target located behind or in the close proximity of natural gas diffusion flames. This measurement is critical for providing high-quality data in structural fire tests. The position of the laser relative to the flame envelope can significantly affect the measurement scatter, but has little influence on the mean values. We observe that the measurement scatter is normally distributed and increases linearly with the distance of the target from the flame along the beam path. Based on these observations, we demonstrate how time-averaging can be used to achieve a standard uncertainty associated with the displacement error of less than 0.1 mm, which is typically sufficient for structural fire testing applications. Measurements with the investigated blue laser sensors were not impeded by the thermal radiation emitted from the flame or the soot generated from the relatively clean-burning natural gas.

Keywords: Position sensor; Displacement; Fire; Blue laser; Structural fire

1   Introduction

Stimulated by the events of September 11th, 2001 and the collapse of the World Trade Center towers, engineering practitioners and policy makers conducted numerous workshops and related studies to identify research, technology and regulatory needs to improve structure performance in the event of a fire [1–6]. Among other needs, these studies recommend increasing efforts to test full-scale structural systems in realistic fires and improving measurement technologies to provide high-quality data from these tests. Displacement measurements are commonly used in large-scale tests of structural systems to assess the structural stability and response to extreme loads. However, typical displacement sensors cannot operate in flames and extreme thermal environments.

McAllister et al. [7] outline the necessary capabilities for displacement sensors based on the expected conditions in structural fire tests. Sensors must function properly in the presence of gas temperatures from 20 °C to 1400 °C for a period up to four hours with known resolution and uncertainty. Meanwhile measurement targets, e.g. a structural steel or concrete member, may experience sustained temperatures up to 750 °C. The measurement method must be insensitive to rapid heating and cooling and it should function in the presence of soot. In the case of displacement, the required measurement range varies based on the object being measured. For example, the range may be small for a bolted connection undergoing thermal expansion or large in the case of sag at the mid-span of a long beam undergoing inelastic deformation. In general, a target measurement range from 1 mm to 1000 mm with a resolution down to 0.1 mm is desirable to assess the behavior of a structure or for control of an experiment.

This paper considers the use of laser triangulation sensors in diffusion flames. Although many optical (noncontact) position measurement techniques exist, laser triangulation sensors are

robust compared to other scientific-grade laser displacement sensors, allow for fast acquisition rates and have a suitable range and accuracy for structural applications [8,9]. Triangulation sensors typically consist of four components: a laser, a collecting lens, a position sensitive detector (PSD) that converts light energy to electrical signal, and signal conditioning electronics. The functional principle of laser triangulation is illustrated in Figure 1. A point of light (continuous or modulated) is projected onto the target surface and the reflection of the light spot passes through a collection lens and is imaged by a detector. The distance to the target can be determined based on the intensity and position of the light received on the detector and geometric relationships. Most triangulation lasers have a fixed "standoff" distance in which no measurements can be made and "measurement range" that are governed by the sensor geometry.
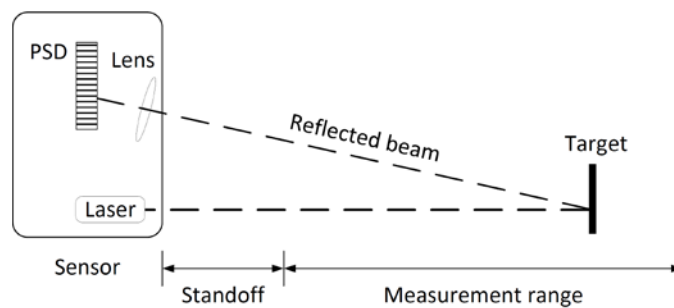
Figure 1 Laser triangulation sensor principle (PSD = Position Sensitive Detector).

Three key impediments to using laser-based displacement sensors in the presence of fire can be summarized as: thermal radiation emitted by the flame and target, refraction of the laser beam by the heated gasses, and extinction of the beam by airborne particulate (e.g., soot).

Laser-based triangulation sensors that operate near the red portion of the electromagnetic spectrum (620 nm to 750 nm) do not work well on glowing targets because the power of the laser signal is overwhelmed by radiation emitted by the "red hot" target. This problem can be overcome by using lasers that operate in the blue-green (350 nm to 570 nm) spectrum. As discussed by Stöbener [10], the required laser power at various wavelengths can be estimated

considering the spectral sensitivity of the detector and the power of the radiation emitted from the heated target as estimated using Planck's law. Alternate technologies for laser-based displacement measurement on hot surfaces, such as time-of-flight lasers [11] and conoscopic holography [12] have also been proposed. Since blue laser triangulation sensors that significantly reduce the problem of target radiation are now commercially available, we do not further consider radiation emitted from a glowing target an impediment. While it is theoretically apparent that lasers operating in the blue-UV spectrum would also have improved performance in the presence of visible radiation emitted from flames (primarily from glowing soot particles), no applications of blue lasers in flames could be found in the literature.

A laser beam in proximity to a flame will be refracted by thermal gradients. This is often referred to as "beam steering". This effect has been used by numerous researchers to study the structure and temperature profile of diffusion flames [13–15]. To the authors' knowledge, no studies have been published that investigate the influence of flame-induced refraction on blue laser triangulation sensors with the purpose of characterizing the position of a target in close proximity to a diffusion flame.

A major impediment to optical measurements in fire is the extinction of the signal by airborne soot particles. Optical extinction coefficients of soot particles in the visible spectrum are well-documented [16–18], and vary according to wavelength, particle size, and particle concentration. Signal loss occurs rapidly for fuels that generate a lot of soot, for example diesel [19]. However, clean-burning fuels such as natural gas generate relatively little soot and are commonly used in large structural fire tests, significantly reducing the problem of laser extinction.

In this paper we report on the feasibility of using blue laser triangulation sensors to measure displacement of a target located behind diffusion flames generated by natural gas. We consider the issue of laser extinction and quantify the effect of laser refraction on the accuracy and uncertainty of the measured displacement. Finally, we show how time-averaging can be used to reduce measurement uncertainty to an acceptable limit in the context of structural fire applications.

2   Experimental setup

The experiments were conducted on an optical table (1.2 m × 2.4 m in plan) located underneath an exhaust hood. The setup consisted of a laser sensor, a burner, a target and barriers to control air currents. Figure 2 shows a photograph of the setup.

Throughout these investigations we used a blue laser triangulation sensor (hereafter "sensor") manufactured by the firm Micro-Epsilon® (model ILD 1700-750BL). The laser uses a blue-violet (405 nm) diode light source operated in pulsed mode with a power less than 1 mW (Class 2 [20]). The measurement range is 750 mm with a start of measurement distance (standoff) of 200 mm from the sensor. The dimensions of the sensor are 150 mm × 80 mm × 35 mm (length × width × thickness). It is noted that while the observations herein can be extrapolated to larger measurement ranges, commercially-available blue triangulation lasers are currently limited to 1000 mm range. This range is adequate for most structural fire engineering applications. We acquired data from a digital output signal at a sample rate of 2500 Hz (the maximum available for this sensor) using the software provided by the manufacturer. The manufacturer-certified linearity over the measurement range (maximum deviation from a straight line) and resolution (smallest change that can be measured) of this sensor under ambient

conditions are 0.75 mm and 0.05 mm, respectively. The distance between the sensor and the fire was sufficient to keep the temperature of the sensor itself well-within its specified operating range.

The burner was a small gas diffusion burner 65 mm in diameter with a silica bead diffusion media. The fuel was natural gas; typically 91 % to 94 % methane, less than 5 % ethane, and less than 1 % propane or other gases (by volume fraction) at our test facility. The gas flow rate was regulated to less than 5 L/min, which produced a flame with a heat release rate and height of less than 4 kW and 350 mm, respectively.

The target consisted of sheet metal painted black, oriented perpendicular to the laser beam and rigidly attached to the optical table. The sensor is insensitive to small target angles [21]. The target and sensor were stationary during each test.

Metal barriers surrounded the setup on three sides during testing; to the left and right of the flame and behind the target. This helped to stabilize the flame against undesired air currents that could push the flame out of the path of the laser.

A schematic drawing of the test setup and geometric variables is provided in Figure 3. Critical variables in the test matrix included: 1) the height of the flame (F_h) as controlled by the gas flow rate (Q), 2) the height of the transmitted (out-going) laser beam (H) relative to the top of the burner, 3) the distance between the flame and the target (D_t) and 4) the total distance between the sensor and the target (D).
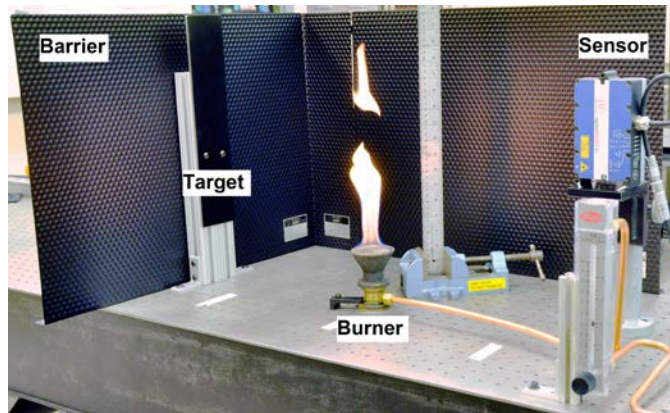
Figure 2 Test setup.
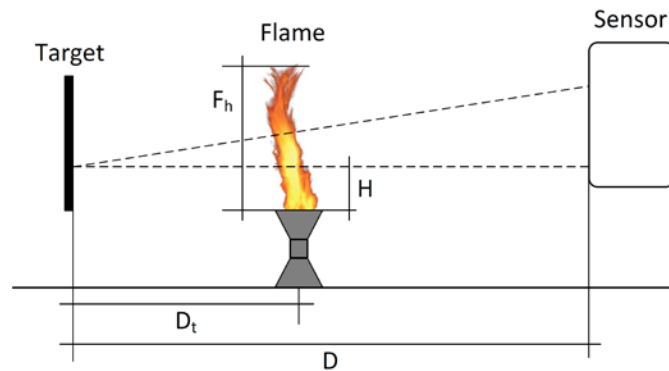
Figure 3 Schematic of test setup illustrating test variables.

3   Results and Discussion

A total of 20 tests were conducted for various configurations of the test geometry and flame size. This section will first present the results for a typical test configuration to demonstrate the common features of the data. Then, the results of several groups of tests will be compared to demonstrate significant influences of diffusion flames on sensor performance as well as data processing requirements specific to this application.

For each test we nominally acquired data for 70 s: 15 s without the burner ignited, followed by 40 s with flame present and finally 15 s after the flame was extinguished. The displacement is shown relative to the initial position measurement, which was determined by the average measurement over the first 10 s of each test. Figure 4(a) shows a typical curve for the resulting

displacement error as a function of time. Referring to the figure, three measurement "zones" were defined for the steady-state conditions before (Zone 1), during (Zone 2), and after (Zone 3) the burn period. The term "displacement error" is used because in the absence of variation inherent to the sensor or induced by the flame, this value should be exactly zero for the stationary target. We determined the start and end times for analysis with flame present (Zone 2) and the start time after the flame was extinguished (Zone 3) based on the times where the standard deviation of a half-second moving window crossed a threshold of 20 % of the maximum observed standard deviation for a given test. We removed the 10 % of the data closest to these boundaries from the zones to mitigate the effect of the burner response time on the results. The specific definition of the zones is arbitrary, but automating the selection allowed for more objective comparison of the data. Figure 4(b)-(d) show frequency histograms generated for the three zones (1, 2, and 3), respectively. The variable N indicates the total number of samples in each zone. Prior to the flame ignition (Figure 4(b)), the displacement error mean (μ) is essentially zero with a standard deviation (σ) smaller than the manufacturer-certified accuracy of 0.05 mm. The measurement variability before the flame is ignited can be attributed to small vibrations of the test setup. With the flame present (Figure 4(c)), the standard deviation increases significantly and a small mean displacement is measured. After the flame is extinguished (Figure 4(d)), the standard deviation decreases significantly, but remains larger than the original value due to the residual thermal gradients above the warm burner. In this example, the mean value of the measurement in Zones 2 and 3 is less than the sensor resolution.
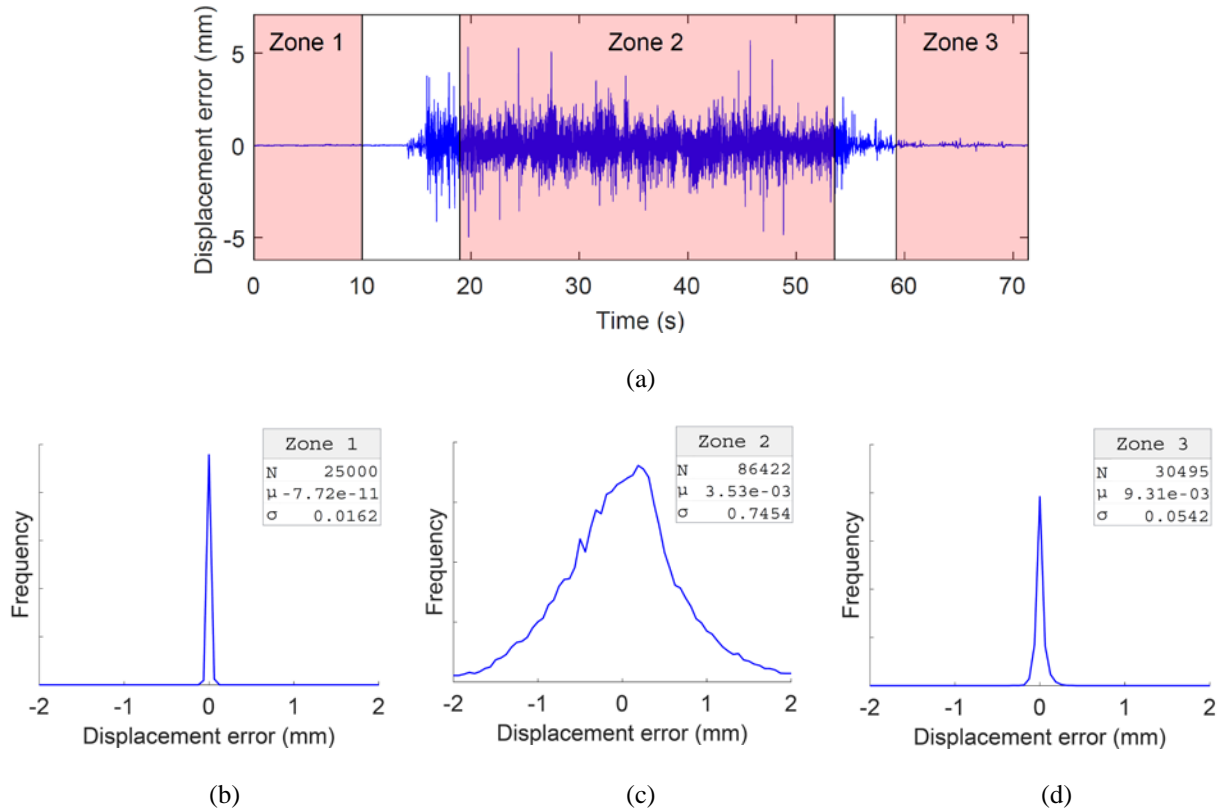
Figure 4 Typical results for the investigated sensor for a stationary target: (a) time-history of the displacement error with processing zones shaded, (b) frequency histogram of the error before flame (Zone 1), (c) frequency histogram of the error during flame (Zone 2), and (d) frequency histogram of the error after flame extinction (Zone 3). (μ and σ in mm)

3.1   Repeatability

To characterize the repeatability of the measurement in the presence of flame (Zone 2), we conducted three test replicates with nominally identical parameters. The gas flow rate (Q) for these tests was set at 3 L/min, resulting in a flame height (F_h) of approximately 300 mm. The laser beam height (H) was 150 mm above the surface of the burner. The burner was located midway between the sensor and the target: $D = 660$ mm and $D_t = 330$ mm. This configuration ensured that the transmitted and return beam paths consistently traveled through the flame.

As described above, the position reading of the sensor was recorded for nominally 40 s while the flame was burning steadily and the measurement error was recorded. Figure 5 shows the frequency distribution of the measurement error for each test, with key distribution

parameters indicated in the inset table. Referring to the figure, the frequency distribution and standard deviation are nearly identical for the three test repeats. The slight variation in the mean values observed between tests is not statistically significant (at 5 % significance level) per one-way analysis of variance (ANOVA). Discussion about downsampling to ensure independence of the data samples is provided in Section 3.5.

The extent to which the data in Figure 5 are normally distributed can be assessed using a quantile-quantile plot (QQ-plot). A QQ-plot is a graphical technique to rapidly determine if two data sets come from populations with a common distribution [22]. In this case, the distribution of the measured displacement error is compared to a normal distribution. If the two data sets come from populations with the same distribution, the results will have a one-to-one ratio. The linearity of the QQ-plots for these data (Figure 6) show that the data are normally distributed for values within approximately two standard deviations of the mean.

Gas flow (Q) = 3 L/min
Laser height (H) = 150 mm
Distance (D) = 660 mm
Target (D_t) = 330 mm

Test	N	μ, mm	σ, mm
Rep 1	86470	-0.0244	1.0042
Rep 2	88762	-0.0039	1.0447
Rep 3	87589	0.0009	1.0576
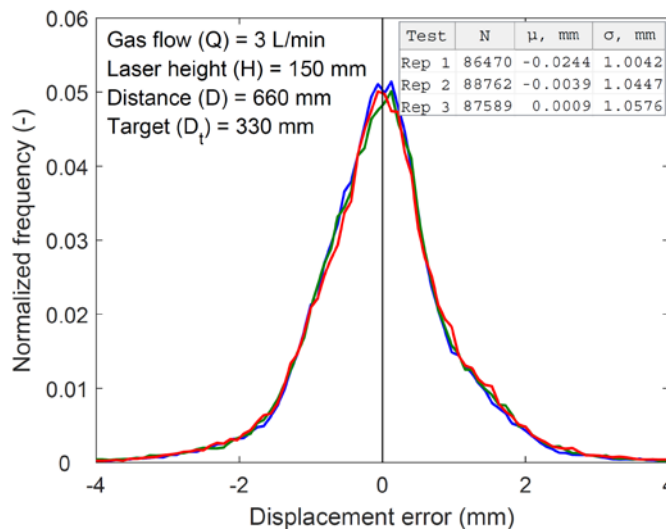
Figure 5 Relative frequency histogram with flame present (Zone 2) for three test repeats.
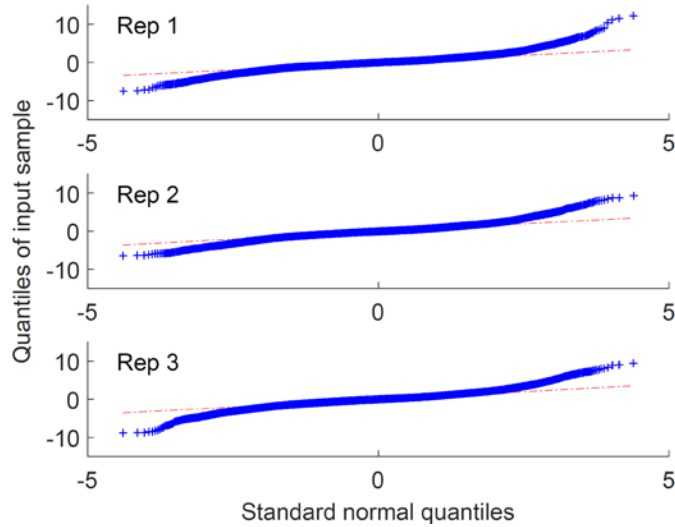
Figure 6 Quantile-quantile plots of the data in Figure 5.

3.2   Laser extinction

As we discussed in the Introduction, a significant impediment to using lasers in a fire environment is the extinction of the signal due to soot. Since in these tests our fuel was natural gas (predominantly methane), the amount of soot generated was small compared to other types of fuel. Nevertheless, we attempted to study the influence of the amount of soot in the path of the laser on the extinction behavior by fixing the laser height (H) at 150 mm and varying the flame size by adjusting the gas flow rate Q. By increasing the flame size, more soot was produced and the length of the laser path through the soot was increased.

Figure 7 shows displacement error time-histories along with corresponding long-exposure images at three different flame sizes. The displacement error time-histories located above the photos in Figure 7 indicate that for this test setup, the increased volume of flames did not prohibit measurement; i.e., there was no detectable loss of signal in the form of outlier values or dropped samples. As this sensor was not inhibited by the maximum fire produced by this burner,

a larger fire is required to study the extinction of signal for the investigated sensor by natural gas flames.

The displacement histories in Figure 7 also illustrate that the majority of the signal noise caused by the flame is due to temperature gradients, rather than by the flame itself (the source of those gradients). The standard deviation of the measurement error without flame (Figure 7(a)) or with flame (Figure 7(b), (c)) in the path of the laser is similar. This observation was further corroborated by the fact that similar standard deviation of the measurement error was observed when the burner was replaced by a small electric heater.

(a)   (b)   (c)
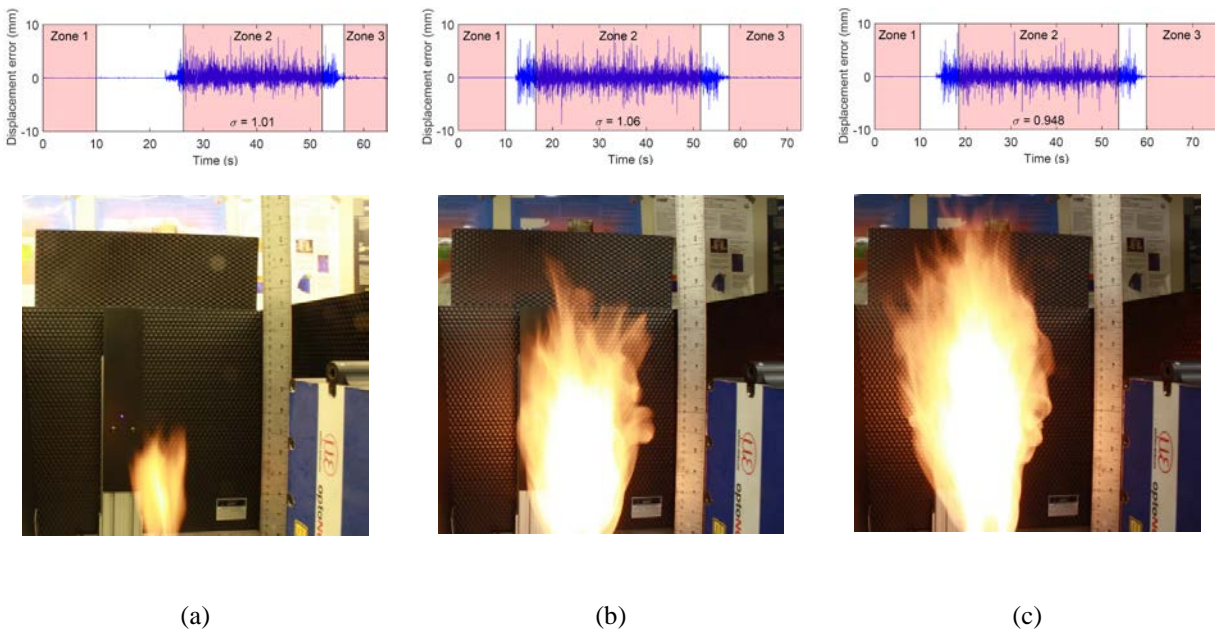
Figure 7 Displacement error time-histories and flame heights as function of gas flow rate (Q): (a) 1 L/min, (b) 3 L/min, and (c) 5 L/min.

3.3   Influence of laser position relative to the flame

To better understand the influence of the thermal field produced by the flame on the measurement, the height of the beam above the burner (H) was varied while the gas flow rate (Q) was held constant at 1 L/min. In these tests, the position of the transmitted beam ranged from well below the flame tip ($H/F_h = 0.33$) to well above the flame tip ($H/F_h = 2.0$). The means and

standard deviations of the displacement error (for Zone 2) are shown in Figure 8. The mean

values of the displacement error are largely unaffected by the position of the beam, however,

there is a small mean offset (< 0.1 mm) when the beam is located above the flame ($H/F_h \geq 1.0$).

The standard deviation is maximized when the transmitted beam is located near the flame tip

($H/F_h = 1.0$). A physical explanation for this behavior is that the (vertical) temperature gradient

and fluctuation is maximized near the tip of the flame. Figure 9 shows the frequency power

spectra resulting from the Fourier transform of the displacement histories corresponding to the

data in Figure 8. When the transmitted and reflected beam paths were located completely within

the flame ($H/F_h = 0.33$ and 0.66), there is a predominant frequency response slightly above

10 Hz. This observation agrees with previous theoretical and experimental studies that show that

"flicker" of diffusion flames has a frequency around 12 Hz [15], [23]. When the beam is at the

flame tip ($H/F_h = 1.0$), the frequency content becomes more broadly distributed between 5 Hz

and 15 Hz. When the laser is completely above the flames ($H/F_h > 1.0$) the frequency content has

no apparent peaks. The loss of the predominant frequency is attributed to turbulent mixing of the

air, and additional randomness in the thermal gradients, above the flame. This understanding of

the frequency content is useful for the time-averaging discussed subsequently in this paper.
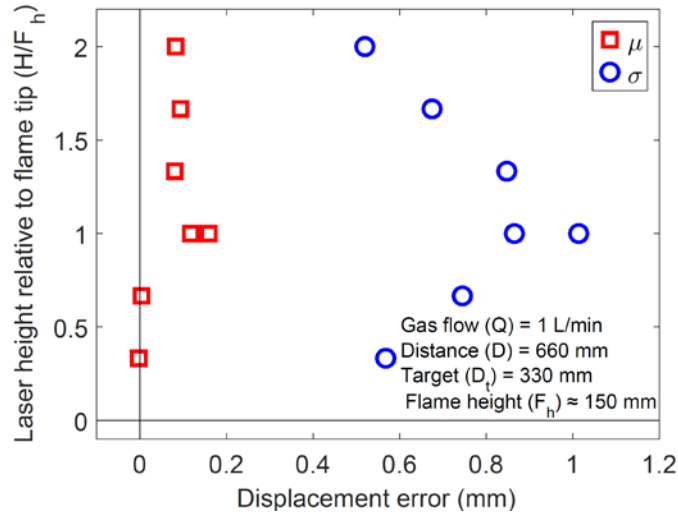
Figure 8 Variation of mean (μ) and standard deviation (σ) of the displacement error as a function of the laser height relative to the flame tip (H/F$_h$).
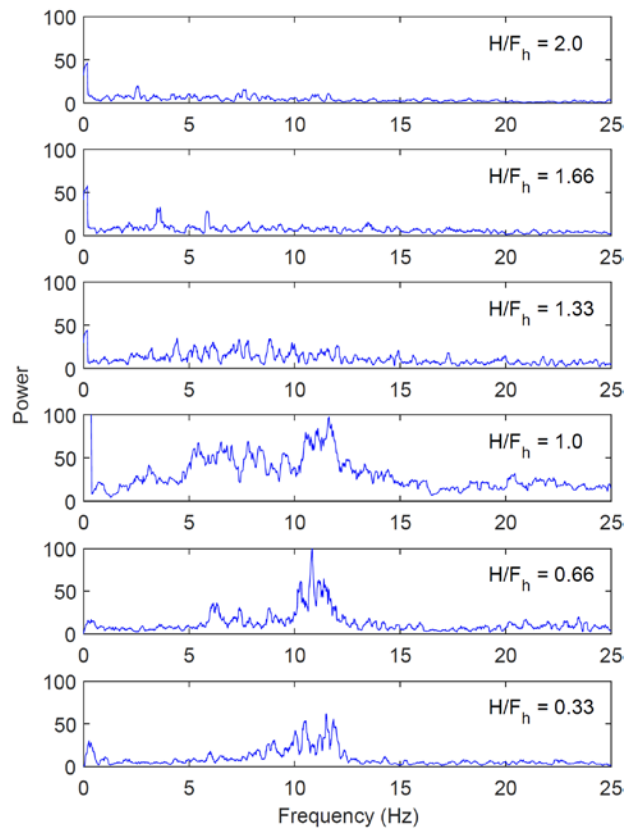
Figure 9 Power spectra for the displacement error time-histories used to generate the data in Figure 8

(only one spectrum for the two test repeats at H/F$_h$ = 1.0 shown for clarity).

3.4   Influence of the flame to target distance

Another factor that significantly influences the performance of the sensor when used through flames is the distance between the flame and the target. Figure 10 shows that the mean of the displacement error is unaffected by the position of the flame along the beam path, however, the standard deviation of the displacement error increases linearly with the flame-to-target distance (D_t). This behavior can be understood by thinking of the flame as a lens – created by a thermal gradient in gas temperature – that refracts the laser beam as the flame flickers. By increasing the distance between the flame and the target, the influence of the refraction increases linearly as illustrated in Figure 11. In Figure 11, only the out-bound laser path is shown for clarity, however, the beam is also refracted on the return path through the flame.
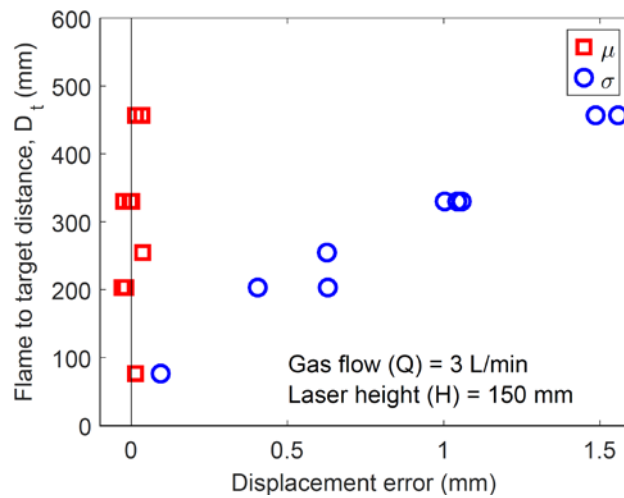
Figure 10Variation of mean (μ) and standard deviation (σ) of the displacement error as a function of the flame-to-target distance (D_t).
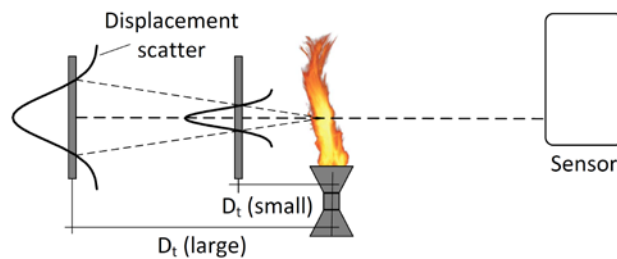
Figure 11Illustration of influence of flame-to-target distance (D_t) on the standard deviation of the measurement.

15 / 21

3.5   Time averaging to reduce measurement uncertainty

As described in the preceding sections, thermal gradients caused by flame induce significant scatter in the measured target position, but the effects are transient. If the physical motion of the measurement target is slow relative to the averaging window length (as is the case in most structural fire testing applications), then time averaging of the signal could effectively reduce measurement uncertainty without significant loss of information about the target position. Figure 12 shows a typical displacement error time history for a stationary target when flame is present in the path of the laser (Zone 2) for raw data sampled at 2500 Hz as well as backward-looking moving averages of the data over 0.1 s (250 samples) and 4 s (10000 samples).
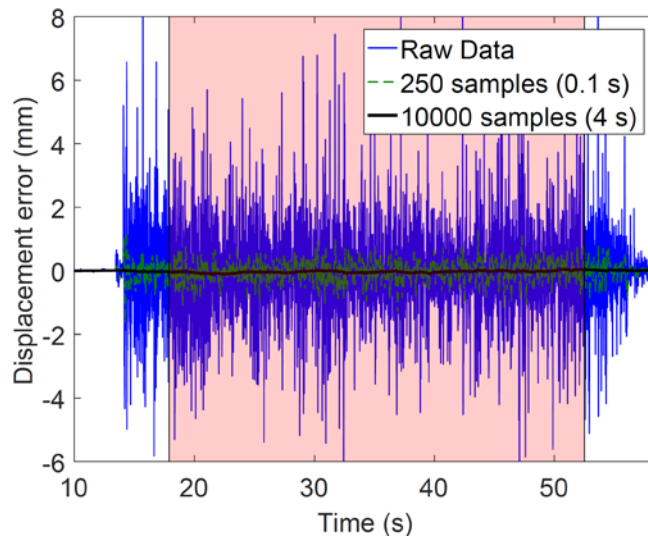
Figure 12: Typical results of investigated blue triangulation laser for a stationary target using moving average window to smooth the data.

Table 1 reports a set of sample statistics of the raw and averaged data from Figure 12. The "Raw" data in Table 1 show that the mean value is a robust indicator, i.e., insensitive to the window length, of the position of the target (due to the lack of outliers in the data). Furthermore, the standard deviation and maximum absolute error (difference between the true position and the recorded value) of these data are reduced by the averaging, as would be expected for largely

normally-distributed data. Because the flame-induced distortion is due to a physical phenomenon with a characteristic time scale, i.e., refraction by the moving thermal gradients, it is useful to look more closely at the independence of the samples for the 2500 Hz sampling rate. To do this, a short section of the time-history response from Figure 12 is shown in Figure 13(a). The autocorrelation plots in Figure 13(b) show the degree of similarity between a sample and the samples around it, i.e., a "lagged" version of itself. At a rate of 2500 Hz, sequential samples are highly correlated to over 300 neighboring samples. Downsampling the data by a factor of 50 (to 50 Hz) reduces the autocorrelation lag length significantly, and consequently reduces the required averaging window length, with negligible change to the mean values or standard deviation (compare "Downsampled" to "Raw" data in Table 1). If the estimated standard deviation of the sensor under normal operating conditions (s_1) is assumed to be ±0.029 mm (sensor resolution of 0.05 mm divided by √3) and the standard deviations resulting from the flames (s_2) are as shown in Table 1, the combined standard uncertainty (u_c) can be calculated as:

$$u_c = \sqrt{\sum_{i=1}^{2} \alpha_i^2 s_i^2} \qquad\qquad Equation\ 1$$

where the sensitivity coefficients are $\alpha_1 = \alpha_2 = 1.0$ [22]. Table 1 shows that the combined standard uncertainty is dominated by the effect of the flames and that it could be reduced below 0.1 mm using a using a window length (t_w) as short as 4 s.

Table 1   Key statistics for shaded zone in Figure 12.

	Displacement error, mm					
	Raw (2500 Hz)			Downsampled (50 Hz)		
Window samples (N_w)	None	250	10000	None	5	200
Window duration (t_w), sec		0.1	4.0		0.1	4.0
Mean (μ)	-0.024	-0.026	-0.029	-0.007	-0.009	-0.016
Standard deviation (σ)	1.004	0.338	0.032	1.023	0.449	0.050
l Maximum l	12.209	1.286	0.112	6.725	2.425	0.147
Combined uncertainty (u_c)	1.004	0.339	0.043	1.023	0.450	0.058
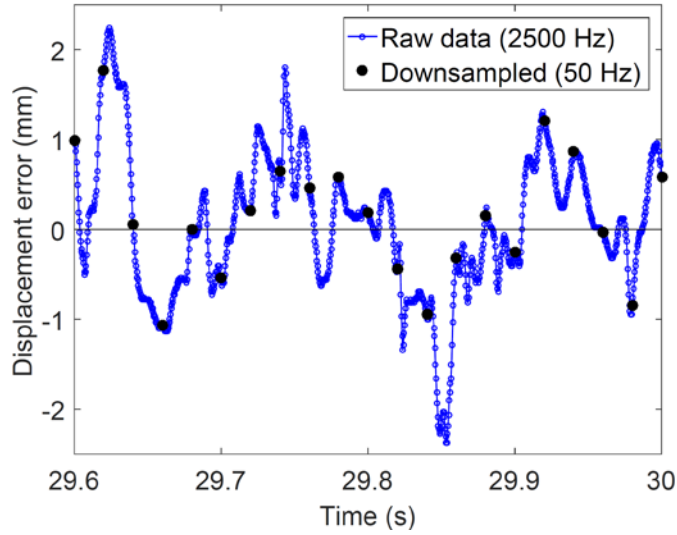
(a)
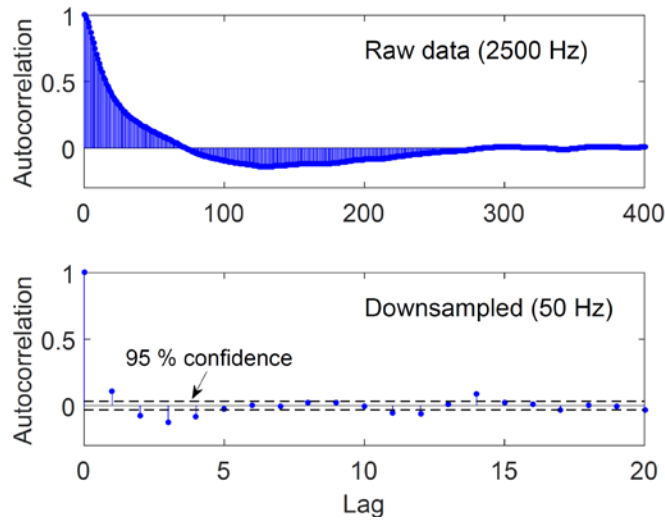
(b)

Figure 13(a) Displacement time-history of raw and downsampled (factor 50) data, and (b) autocorrelation of raw and downsampled data (for Zone 2).

When structural member displacement is measured in a real application, the mean displacement will typically vary (slowly) with time as the member and structure deform. Therefore, application of averaging must be applied appropriately for a non-stationary process. The window length must be sufficiently short to capture salient transient features in the mean displacement but long enough to ensure that the uncertainty of the mean of the window is below

the desired threshold. Selecting the appropriate window length can be done manually during post-processing by taking into account the above observations.

4   Summary, conclusions and future work

Researchers need improved methods to accurately make displacement measurements in building fire experiments. The harsh conditions in a building fire – rapidly fluctuating gas temperatures up to 1400 °C, radiation emitted from flames and heated targets, and the presence of soot – challenge technologies that have been developed to measure displacement under ambient conditions. This study explores the feasibility of using commercially-available blue laser triangulation sensors to measure displacement of targets located behind or in the close proximity of diffusion flames generated by natural gas.

The results suggest that blue laser triangulation sensors are promising for this application. The soot present in and above the small (< 4 kW) diffusion flames did not measurably decrease the signal strength of the investigated sensor. Distortion of the measurement by the thermal gradients when the laser beam passed near the flame was significant, but largely normally distributed around the true value. The standard deviation of the measurement was highest when the beam passed close to the edge of the flame, and increased linearly with the distance between the flame and the measurement target. The mean value of the measurement was altered slightly when the beam passed above the flame, but generally remained very low. Because typical targets in a structural fire test move slowly relative to the measurement distortion caused by the flame, time-averaging of the results can be used to achieve a representative mean value of the target displacement. For the small diffusion flame studied in this test, a moving average filter 4 s long provides an estimate of the target displacement with a standard uncertainty near the resolution threshold of the investigated sensor.

Based on these results, we recommend additional testing to verify functionality of this laser type in larger natural gas fires where the entire laser beam travel path is engulfed by flame. Work is recommended to study optimized windowing methods that can be used to efficiently track non-stationary targets. These methods must account for the temporal variation characteristics of building movement in a fire and the influence of fire dynamics on measurement distortion. Finally, for practical application, cooling enclosures that allow a sensor to be placed within a burning room in close proximity to structural members need to be developed.

Disclaimer

This work was funded by the National Institute of Standards and Technology (NIST). Certain commercial equipment, instruments, or materials are identified in this paper in order to specify the experimental procedure adequately. Such identification is not intended to imply recommendation or endorsement by NIST, nor is it intended to imply that the materials or equipment identified are necessarily the best available for the purpose.

References

[1] Grosshandler W 2002 *Fire Resistance Determination and Performance Prediction Research Needs Workshop: Proceedings (NIST IR 6890)* (Gaithersburg, MD)

[2] Beitel J and Iwankiw N 2008 *Analysis of Needs and Existing Capabilities for Full-Scale Fire Resistance Testing (NIST GCR 02-843-1)* (Gaithersburg, MD)

[3] Almand K 2012 *Structural: Structural Fire Resistance Experimental Research - Priority needs of U.S. Industry (NIST GCR 12-958)* (Gaithersburg, MD)

[4] Kodur V K R, Garlock M and Iwankiw N 2012 Structures in Fire: State-of-the-Art, Research and Training Needs *Fire Technol.* **48** 825–39

[5] Bisby L, Gales J and Maluk C 2013 A contemporary review of large-scale non-standard structural fire testing *Fire Sci. Rev.* **2** 1–27

[6] Yang J C, Bundy M F, Gross J L, Hamins A P, Sadek F H and Raghunathan A 2015 *International R and D Roadmap for Fire Resistance of Structures Summary of NIST/CIB Workshop (NIST SP 1188)* (Gaithersburg, MD)

[7] McAllister T, Luecke W, Iadicola M and Bundy M 2012 *Measurement of Temperature,*

Displacement, and Strain in Structural Components Subject to Fire Effects: Concepts and Candidate Approaches (NIST TN 1768) (Gaithersburg, MD)

[8]   Berkovic G and Shafir E 2012 Optical methods for distance and displacement measurements *Adv. Opt. Photonics* **4** 441

[9]   Amann M-C, Bosch T, Lescure M, Myllyla R and Rioux M 2001 Laser ranging: a critical review of usual techniques for distance measurement *Opt. Eng.* **40** 10–9

[10]   Stöbener D, Dijkman M, Kruse D, Surm H, Keßler O, Mayr P and Goch G 2003 Distance Measurements With Laser-Triangulation in Hot Environments *Proceedings, XVII IMEKO World Congress* pp 1898–902

[11]   Määtta K, Kostamovaara J and Myllylä R 1993 Profiling of hot surfaces by pulsed time-of-flight laser range finder techniques *Appl. Opt.* **32** 5334–47

[12]   Álvarez I, Enguita J M, Frade M, Marina J and Ojea G 2009 On-Line Metrology with Conoscopic Holography: Beyond Triangulation *Sensors* **9** 7021–37

[13]   Shakher C and Nirala A K 1999 A review on refractive index and temperature profile measurements using laser-based interferometric techniques *Opt. Lasers Eng.* **31** 455–91

[14]   Chang H and Charalampopoulos T T 1990 Determination of the Wavelength Dependence of Refractive Indices of Flame Soot *Proc. R. Soc. A Math. Phys. Eng. Sci.* **430** 577–91

[15]   Ballantyne A and Bray K N C 1977 Investigations into the structure of jet diffusion flames using time-resolved optical measuring techniques *Symp. Combust.* **16** 777–87

[16]   Zhu J, Choi M Y, Mulholland G W, Manzello S L, Gritzo L a. and Suo-Anttila J 2002 Measurement of visible and near-IR optical properties of soot produced from laminar flames *Proc. Combust. Inst.* **29** 2367–74

[17]   Dobbins R A, Mulholland G W and Bryner N P 1994 Comparison of a fractal smoke optics model with light extinction measurements *Atmos. Environ.* **28** 889–97

[18]   Colbeck I, Atkinson B and Johar Y 1997 The morphology and optical properties of soot produced by different fuels *J. Aerosol Sci.* **28** 715–23

[19]   Maranghides A, William M, Walton W D, Johnsson E L and Bryner N P 2006 *Free Space Optics Communication System Testing in Smoke and Fire Environments National Communications System (NIST IR 7313)* (Gaithersburg, MD)

[20]   International Electrotechnical Commission 2014 IEC 60825-1:2014: Safety of laser products - Part 1: Equipment classification and requirements 220

[21]   MicroEpsilon Messtechnik 2015 Instruction Manual: optoNCDT 1700

[22]   National Institute of Standards and Technology NIST/SEMATECH e-Handbook of Statistical Methods, http://www.itl.nist.gov/div898/handbook, Accessed: January 2016

[23]   Buckmaster J and Peters N 1988 The infinite candle and its stability—A paradigm for flickering diffusion flames *Symp. Combust.* **21** 1829–36